# β-Relaxation and low-temperature specific heat in (KBr)1-x(KCN)x

**B. Mertz, R. Böhmer, B. Eisele, Alois Loidl**

**Angaben zur Veröffentlichung / Publication details:**

Mertz, B., R. Böhmer, B. Eisele, and Alois Loidl. 1990. "β-Relaxation and low-temperature specific heat in (KBr)1-x(KCN)x." *Zeitschrift für Physik B: Condensed Matter* 79 (3): 431–40. https://doi.org/10.1007/bf01437654.



# $\beta$-Relaxation and low-temperature specific heat in $(KBr)_{1-x}(KCN)_x$

**B. Mertz, R. Böhmer[1], B. Eisele, and A. Loidl**

Institut für Physik, Johannes-Gutenberg Universität, Mainz, Federal Republic of Germany

The specific heat in $(KBr)_{1-x}(KCN)_x$ has been measured for concentrations $0.00 \leqq x \leqq 0.93$ and for temperatures $2\,K \leqq T \leqq 50\,K$. In addition, the dipolar relaxation phenomena were studied using dielectric spectroscopy. The relaxation behaviour was parametrized assuming a Gaussian distribution of energy barriers and the mean activation energies, the distribution widths, and the attempt frequencies have been determined as a function of the $CN^-$ concentration. With these parameters the linear and the excess specific heat contributions were calculated and compared to the calorimetric results.

## I. Introduction

Orientational glasses are crystalline materials which transform from a high-$T$ crystalline phase into a low-$T$ glass state [1]. Analogous to spin glasses, randomly substituted impurity atoms are located on a topologically ordered lattice. At high temperatures the orientational degrees of freedom are dynamically disordered. Below the glass transition the orientational disorder is frozen-in due to frustrated interaction forces. As a prominent example, $(KBr)_{1-x}(KCN)_x$ exhibits an orientational glass state in a wide concentration range ($0.10 \leqq x \leqq 0.6$) [1, 2]. Here the relaxation phenomena and the structural properties resemble those of an amorphous state at low temperatures [1]. For example the relaxational phenomena associated with the dipolar and quadrupolar degrees of freedom mimic properties as observed in canonical glasses. Specifically, the freezing of the elastic quadrupole moments corresponds to a structural ($\alpha-$) relaxation, whereas the dipolar slowing down can be viewed as a secondary ($\beta-$) process [3, 4]. In addition, the low-temperature ($T \leqq 1$ K) thermodynamic [5], elastic [6] and dielectric properties [7, 8] are characteristic of amorphous systems. Taking into account the model character of the cyanide glasses, Sethna et al. [9–11] proposed a microscopic theory which relates the low-temperature thermodynamic behaviour to the high-temperature dielectric relaxation.

An outstanding feature of the solid solutions of alkali halide and alkali cyanide compounds is the glassy low-temperature specific heat $C_p$ [5]. In amorphous systems $C_p$ can be described by [12]

$$C_p = C_1(t)\,T^{\alpha} + C_{\text{exc}}\,T^3 + C_D\,T^3, \tag{1}$$

with $\alpha \approx 1$. The first term depends logarithmically on time and is roughly linear in temperature. $C_D$ characterizes the normal Debye specific heat of an insulating crystal. Finally, $C_{\text{exc}}$ gives rise to an excess contribution to the specific heat, which follows a $T^3$ dependence in a limited temperature range ($T \lesssim 2$ K) [13]. These contributions to the specific heat are universal features of the glassy state [12]. The linear term has been interpreted in terms of a tunneling model by Anderson, Halperin and Varma [14] and by Phillips [15]. Assuming a constant density of tunneling states, these authors were able to calculate the experimentally observed temperature and time dependences. For most of the glassy solids the nature of the tunneling motion is still unknown. Attempts have been made to identify the tunneling entity for certain materials. As an example, Buchenau et al. [16] proposed the coupled motion of neighbouring molecules to be responsible for the thermal anomalies in vitreous silica.

Less is known about the anomalous $T^3$-term in the specific heat. This term is not time dependent and therefore seems not to be related to the tunneling states [17, 18]. A variety of possible explanations for the occurrence of $C_{\text{exc}}$ has been suggested:

– extra localized modes which were assumed to be characteristic of the glassy phase [19].

– low lying librational modes of coupled $SiO_4$ tetrahedra [16] whose tunneling motion was suspected to lead to the linear term at $T < 1$ K.

– the crossover from sound wave propagation at low frequencies to the vibration of fractals [20].

[1] *Present address*: Department of Chemistry, Arizona State University, Tempe, AZ 85287, USA

– the mixing of large wave vector components into the low frequency transverse modes yielding an additional contribution to the vibrational density of states [21].
– soft surface phonons of partially polymerized clusters which were assumed to be intrinsic to the glass state [22].
– a density of tunneling states that decreases exponentially for large energy splittings [23]. However, this prediction seems to be in conflict with the time independence of the $C_{exc}$-contribution observed experimentally [17, 18].

Very recently a new approach has been developed by Schirmacher and Wagener [24]: they showed that the anomalous behaviour of the specific heat in glasses is a direct consequence of disorder. Following their ideas, the excess contribution to the specific heat results from a crossover of free sound wave propagation to a regime where the sound waves are heavily damped.

Taking advantage of the topological order and of the fact that at low temperatures the molecular reorientations in the cyanide glasses are dominated by the dipolar degrees of freedom, Sethna et al. [9] proposed a microscopic model. Here the linear term in the specific heat can be calculated from the $180^0$ tunneling flips of the cyanide molecules. The tunneling takes place in the Born-Mayer potentials of the surrounding $K^+$ ions being essentially defined by the quadrupolar interaction forces. Or to be more specific, the tunneling motion probes the local crystal field due to frozen-in shear strains. Thus, the dipolar relaxation at high temperatures and the tunneling excitations for $T \lesssim 2$ K are governed by the same distribution of hindering barriers and dielectric measurements can be utilized to determine the crystal field parameters.

Later on, it was supposed [10] that the excess specific heat in $(KBr)_{1-x}(KCN)_x$ can be explained by librational modes of the $CN^-$ dumbbells within the hindering barriers mentioned above. The plateau in the thermal conductivity in the cyanide glasses, another common signature of glassy materials, was treated within the framework of the same model. Consequently, $(KBr)_{1-x}(KCN)_x$ was assumed to be a unique model system [9–11] where it is possible to calculate the linear and the excess term of the specific heat from parameters as determined by dielectric spectroscopy of the $\beta$-relaxation.

The aim of this work was to verify experimentally the predictions of Sethna et al. [9–11] concerning the linear term and the excess contribution of the specific heat. Subsequent to the pioneering work of Lüty [2], dielectric investigations in $(KBr)_{1-x}(KCN)_x$ have been performed by a number of experimentalists [25–27]. Using dielectric data for $x=0.25$, 0.5 and 0.7 Wu et al. [28] and Ernst et al. [28] have calculated the linear term $C_1(t)$ according to Sethna's model and found good overall agreement with the experimental specific heat results [5]. The linear term of the specific heat has been investigated in detail for different concentrations $x$ in $(KBr)_{1-x}(KCN)_x$ by De Yoreo et al. [5]. Very recently Watson et al. have reported specific heat data for $(KBr)_{1-x}(KCN)_x$ mixed crystals with $x=0.19$, 0.41 and 0.60 [29].

Here we present the results of a series of dielectric investigations performed in the complete concentration range. In addition, calorimetric data have been collected for concentrations $x=0.00$, 0.008, 0.05, 0.15, 0.23, 0.46, 0.53, 0.65, 0.73 and 0.93 and for temperatures $2\text{ K} \leqq T \leqq 50$ K. From these data the Debye and the excess term of $C_p$ have been determined unambiguously. Within the framework of the microscopic model we calculate the linear and the excess contribution to the specific heat from the parameters as evaluated from the dielectric dispersion. For this purpose the mean hindering barriers, the distribution widths of the barriers and the attempt frequencies are deduced from our dielectric measurements. The results are compared to the experimentally observed low-temperature specific heat.

## II. Models for the low-temperature specific heat

### A. *The linear term*

Within Sethna's model the prefactor of the linear term $C_1(t)$ from (1) is given by [9]

$$C_1(t)=\frac{\pi^2}{6} k_B^2 P(t). \tag{2}$$

In the standard tunneling model the assumption is made that the distribution of tunneling states $P(\Delta, E)$ is independent of the asymmetry energy $\Delta$, i.e.

$$P(\Delta, E)=n_0 P(E) \tag{3}$$

with $n_0=1/\Delta$ [9]. The number of tunneling states per mole and unit energy that can tunnel within an experimental time $t$ can be calculated from the dielectric data [9] by:

$$P(t)=\frac{xN_L}{\Delta}\int_0^\infty D(E)\,[1-\exp(-\Gamma(E)\,t)]\,\mathrm{d}E. \tag{4}$$

Here $D(E)$ represents a Gaussian distribution of energy barriers and $\Gamma(E)$ denotes the tunneling rate through a barrier of height $E$ [9]. In $(KBr)_{1-x}(KCN)_x$ the tunneling rate $\Gamma(E)$ of the $CN^-$ dipoles is given by [9]

$$\Gamma(E)=\Gamma_0 \exp[-4\sqrt{2IE}/\hbar]. \tag{5}$$

Here a sinusoidal potential has been assumed where the minima correspond to orientations of the $CN^-$ dumbbells which are separated by $180^0$. The moment of inertia of the of CN molecule is given by $I=2.65\ 10^{-39}$ g cm$^2$ [30] and $\Gamma_0$ is the attempt frequency.

Using Eqs. (2)–(5) the linear term in $(KBr)_{1-x}(KCN)_x$ can be calculated with only one free parameter, namely $\Delta$. For pure KCN the asymmetry was evaluated from dielectric data to be $\Delta/k_B=340$ K [28]. As a first approximation $\Delta$ was assumed to be independent of concentration [9, 28]. With these assumptions the low-temperature specific heat in the cyanide glasses can be computed for all concentrations without adjustable parameters.

*B. The excess term at intermediate temperatures*

All glassy materials exhibit an excess contribution to the specific heat in an intermediate temperature regime which appears as a bump in a $C/T^3$ versus $T$ plot [12]. This anomalous heat capacity of amorphous materials coincides with the $T$ independence of the thermal conductivity and a number of theoretical work treat both phenomena within the same models.

Randeria and Sethna [10] identified the excess contribution to the specific heat in $(KBr)_{1-x}(KCN)_x$ as originating from single particle librational excitations of the $CN^-$ ions. Following handwaving arguments, the librational frequency $\omega_{lib}$ in a parabolic potential is given by

$$\omega_{lib}(x)=\sqrt{2E_0(x)/I_{eff}}. \tag{6}$$

Here $E_0(x)$ is the mean barrier height for a given $CN^-$ concentration, and $I_{eff}$ is an effective moment of inertial of the $CN^-$ molecule. Equation (6) defines a mean librational frequency $\omega_{lib}(x)$. A distribution of hindering barriers can be transformed into a distribution of librational states. Its full width at half maximum (FWHM) $\sigma_{lib}$ is given by

$$\sigma_{lib}=\sigma\frac{\omega_{lib}}{2E_0}. \tag{7}$$

The mean barrier height and the FWHM of the Gaussian distribution of barriers were determined from the dielectric measurements of this work.

Later on, Grannan et al. [11] improved this model and introduced a modified density of states via a coupling of librational and translational modes.

## III. Experimental results

Most of the $(KBr)_{1-x}(KCN)_x$ single crystals used for this work have been grown by S. Haussühl of the Universität zu Köln. Mixed crystals with concentrations $x=0.41$ and 0.23 were purchased from the Crystal Growth Laboratory of the University of Utah. Detailed specific heat and dielectric studies have been performed on crystals with actual $CN^-$ concentrations $x=0.00$, 0.008, 0.05, 0.15, 0.23, 0.41, 0.46, 0.53, 0.65, 0.73 and 0.93. The concentrations were determined gravimetrically [31].

*A. Dielectric investigations*

For the dielectric measurements thin crystal plates, typically $1*1*0.1$ cm$^3$ in size, were cleaved along the {100} planes from optically clear parts of the mothercrystals. The slabs were inserted in stress free configuration between the electrodes of a guard ring capacitor, covering an active area of approximately 4.1 cm$^2$. To prevent chemical reactions of the cyanide samples with the copper electrodes, the crystals were sandwiched with 50 μm thick Mylar foil. The capacitance and conductance of the assembly was monitored with a HP4274A multifrequency LCR-meter in a four wire configuration. An excitation voltage of 5 $V_{rms}$ was employed througout the frequency range from 100 Hz to 100 kHz. Using these fields the response is still linear [25, 26]. The complex dielectric constant $\varepsilon=\varepsilon'-i\varepsilon''$ was computed from the measured impedance with an error amounting up to 10% of the absolute $\varepsilon$-value. This large uncertainty arises from a rather unprecise determination of the sample geometry, but it does not affect the shape of the dielectric spectra which contains all the information to be presented below. Depending on the measuring frequency the relative error was at least one order of magnitude smaller as compared to the absolute one. Temperatures between 3 K and 300 K were measured with a calibrated diode sensor with an accuracy better then $\pm 0.5$ K for $T<100$ K and $\pm 1$ K above. Due to the relatively large mass of the capacitor a temperature stability of always better than 0.1 K was easily maintained during a complete frequency sweep.

As commonly found in mixed cyanides, the dielectric spectra were symmetrically shaped, when plotted on a logarithmic frequency scale. The rather broad dielectric losses $\varepsilon''(\lg\omega)$ [32] and the smeared out steps of the dielectric constant $\varepsilon'(\lg\omega)$ [32] were fitted with a distribution of relaxation times in combination with an Arrhenius law

$$\tau=\tau_0\exp(E/k_B T). \tag{8}$$

Here $\tau$ is the relaxation time, $E$ the energy barrier that has to be crossed by the thermally activated dipoles, and $\Gamma_0=1/(2\pi\tau_0)$ is being called the attempt frequency. To describe broad dielectric loss curves, $\tau_0$ or $E$ (or both) can be distributed. The Cole-Cole approach [33] which merely distributes the prefactor $\tau_0$, fits the $\varepsilon$ data as well as does a model that assumes a Gaussian probability density for the hindering barriers $E$. For a comparison of the dielectric data with the results of the specific heat experiments the parametrization in terms of a distribution of energy barriers seems to be more appropriate. It leads to an expression that must be evaluated numerically [27].

$$\varepsilon=\varepsilon_\infty+\frac{(\varepsilon_s-\varepsilon_\infty)}{\sigma'\sqrt{2\pi}}\int_0^\infty\frac{\exp\{-(E-E_0)^2/(2\sigma'^2)\}}{1+i\omega\tau(E)}\,dE. \tag{9}$$

The dielectric constant in the high-frequency limit $\varepsilon_\infty$ and the dispersion step $(\varepsilon_s-\varepsilon_\infty)$ are of less interest here. Thus, our main interest is focused on the dipole concentration dependence of the attempt frequency $\Gamma_0$, the center of the Gaussian $E_0$, and its full width at half maximum (FWHM) $\sigma=\sigma' 2\sqrt{2\ln 2}$. Good fits were obtained allowing of a weak temperature dependence of $\sigma$ as discussed below. The attempt frequencies which result from these fits are shown in Fig. 1. Starting from diluted samples, $\Gamma_0$ increases strongly with increasing dipole concentration $x$ and remains almost constant for $x>0.4$, in accordance with published values [28]. For higher concentrations the estimated values of $\Gamma_0$ are two decades higher than the librational frequencies, which

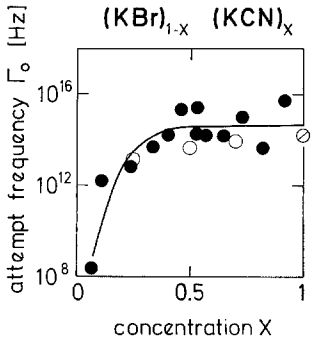


**Fig. 1.** Attempt frequencies in $(KBr)_{1-x}(KCN)_x$ as determined from dielectric measurements: this work (●), Ref. 35 (⊘) and Ref. 28 (○). The line is drawn to guide the eye

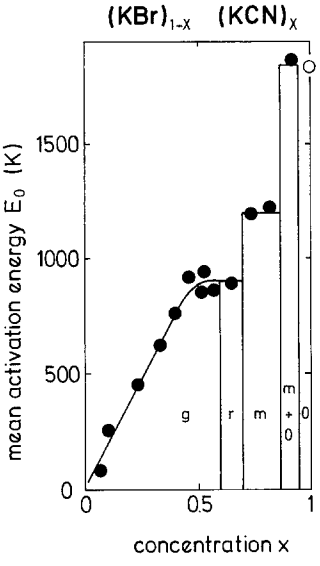


**Fig. 2.** Mean hindering barriers $E_0(x)$ for dipolar reorientations: this work (●); Ref. 35: (○). The vertical lines are schematic representations of the phase boundaries between glassy cubic (*g*), glassy rhombohedral (*r*), monoclinic (*m*) and orthorhombic (*o*) phases

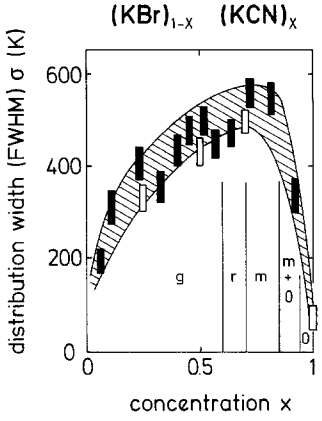


**Fig. 3.** Width (FWHM) of the Gaussian distributions of energy barriers for different $CN^-$ concentrations. The vertical extension of the bars indicates the variation of $\sigma$ with temperature: this work (■); Ref. 28: (□). The value for pure KCN was taken from Ref. 35. The hatched area emphasizes the concentration and temperature dependence of $\sigma$. Vertical lines indicate phase boundaries as in Fig. 2

can be viewed as the 'true' attempt frequencies in these crystals [34]. Under the assumption that the energy barriers decrease linearily with temperature, $\Gamma_0$ was shown to approach reasonable values [28].

At first glance, the mean activation energies $E_0(x)$, depicted in Fig. 2 exhibit a linear increase with $x$. At very low concentrations $E_0$ reflects the crystal field acting on the $CN^-$ molecule in the octahedral environment of the cubic KBr host-lattice. In pure KCN the barriers against reorientation are essentially determined by the Born-Mayer potential of the elastically ordered phase. A closer inspection shows that the energy barriers in crystals with orthorhombic or monoclinic low-$T$ phases differ significantly from samples which exhibit a rhombohedral or a pseudo-cubic glassy low-temperature state. For low concentrations $E_0$ scales almost linearly with $x$. This indicates that the dipoles experience a potential determined by the quadrupolar interaction forces [34] where the dipolar relaxation probes the local environment which locally exhibits strong deviations from cubic symmetry due to the quadrupolar freezing transition. Another remarkable feature is that near the critical concentration $x_c$ in the cubic and in the rhombohedral phases comparable mean activation energies were found.

Reasonable fits to the dielectric data were obtained with a temperature independent width. They could be improved considerably, if a variation for different temperatures was permitted, in magnitude similar to the one observed by other experimentalists [27, 28]. The concentration dependence of the width parameter is shown in Fig. 3. In this figure the observed temperature dependence of the width parameter is indicated by the height of the bars. Surprisingly, the width of the distribution of barrier heights $\sigma(x)$ is largest for crystals in the monoclinic phases, while the widths of the corresponding dielectric loss curves do not exceed the ones for crystals near the critical concentration. Due to the higher barriers in the monoclinic samples the dielectric loss maxima for a given frequency shift to higher temperatures. This is quantitatively accounted for by the empirical relation $\sigma \sim WT$, with $W$ being the width of $\varepsilon''(\lg(f))$ or the width of a distribution of relaxation times [36]. As expected, the distribution widths approach values near zero for crystals where random potentials are essentially absent. These random local fields are responsible for the large $\sigma$-values at intermediate concentrations.

### *B. Specific heat measurements*

Cubes of approximately 1 $cm^3$, cleaved from large crystals, were used as samples. The molar specific heat of the crystals was measured by the quasi-adiabatic Nernst method using a standard calorimeter. Joule heat was applied to the sample by means of a heater wire directly attached to the sample surface with varnish (Ge 7031). The temperature was measured with a Germanium

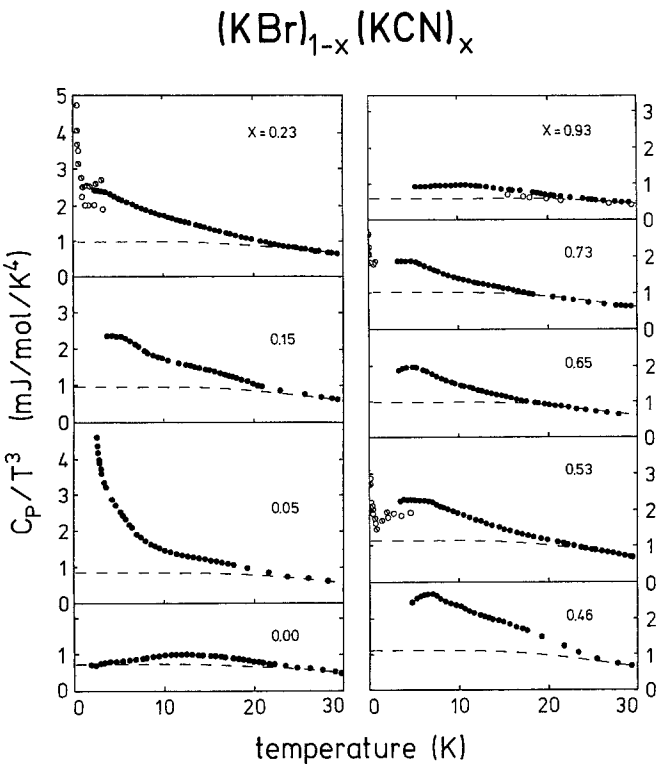


**Fig. 4.** Specific heat plotted as $C_p/T^3$ versus $T$ for concentrations $x=0.00$, 0.05, 0.15, 0.23, 0.46, 0.53, 0.65, 0.73, and 0.93. The Debye specific heat is represented by the dashed lines. Data taken from literature are subjoined in some cases: for $x=0.23$ data meet those taken from Ref. 7 (○, $x=0.20$) and from Ref. 5 (⊙, $x=0.25$), for $x=0.53$ data are added taken from Ref. 5 (⊙, $x=0.50$) and Ref. 7 (○, $x=0.50$). The results for $x=0.73$ are depicted together with those for $x=0.70$ taken from Ref. 5 (⊙). In the case of $x=0.93$ the open circles indicate results for $x=1.00$ after Ref. 39

($2\,\mathrm{K} \leqq T \leqq 40\,\mathrm{K}$) or a Platinum resistor ($10\,\mathrm{K} \leqq T \leqq 50\,\mathrm{K}$), respectively, using a four wire arrangement with a resistance bridge employing the lock-in technique. The obtained temperature versus time profiles were analyzed by a fully computerized control and data acquisition system. Errors of the $C_p$-values are smaller than 5%.

Figure 4 shows representative results of the specific heat measurements for selected concentrations plotted as $C_p/T^3$ versus $T$ [37]. This representation emphasizes the excess specific heat appearing as a bump above the normal Debye contribution $C_D$. Below 1 K $C_p/T^3$ rises rapidly due to the linear term in $C_p$. This is documented here by data taken from literature [5, 7]. The dashed lines in Fig. 4 show the calculated Debye specific heat, caused by the pure phonon contributions of the center of mass lattices. For pure KBr the extra specific heat near 12 K is thought to be due to a high density of transverse acoustic phonons near the zone boundary [38]. For $x=0.05$ the strong increase towards 0 K indicates a strong non-Debye specific heat at low $T$. Obviously, for this concentration excess and linear contributions to the specific heat merge. This behaviour may result from a discrete spectrum of tunneling and librational excitations which is broadened through the strain mediated interactions between neighbouring $CN^-$ dumbbells. We try to give a more quantitative description later. For $x=0.93$, $C_p(T)$ closely follows the Debye specific heat expected for crystalline solids (values for pure KCN [39] are indicated).

The $C_{exc}$ contribution at intermediate temperatures looks similar for all concentrations $0.1 \leqq x \leqq 0.8$. This regime covers the cubic and rhombohedral glassy state as well as the monoclinic phase. Obviously the behaviour which resembles that of a glass shows up even in the ordered phases. The bump in Fig. 4 exhibits only a weak temperature dependence. At first glance, these experimental observations are in conflict with the predictions of Sethna's theory [10, 11]. From the model calculations we expect a shift of the bump of the specific heat towards higher temperatures with increasing concentrations. This is a consequence of (6) which shows that the librational energies scale with the square-root of the hindering barriers, which in turn increase almost linearly with increasing concentration (Fig. 2).

## IV. Analysis and discussion

To achieve a more quantitative comparison of our experimental results with the theoretical predictions, we tried to fit the observed excess specific heat at intermediate temperatures using a distribution of Einstein modes which is thought to be due to a distribution of librational energies. However, before performing a detailed analysis, it seems worthwhile to collect the experimental facts concerning the rotational excitation spectrum of the $CN^-$ dumbbell in the crystal field of the host lattice.

### *A. The rotational excitation spectrum*

The rotational excitation spectrum of the mixed cyanides includes tunneling and librational excitations. It has been studied in full detail using inelastic neutron scattering [40–42] and Raman techniques [43]. Focusing on $(KBr)_{1-x}(KCN)_x$, we note that in the dilute limit a tunneling transition in $T_{2g}$ symmetry has been detected near 3 K by Rowe et al. [41] and by Loidl et al. [42]. A librational transition in $E_g$ was found near 15 K [41, 42]. For concentrations $x>0.01$ tunneling transitions were not observable due to the strong rotation-translation coupling which acts as an indirect effective interaction between the tunneling centers. It is well known that in a local strain field the tunneling transition energies increase and are smeared out with increasing strain amplitudes [44]. Librational excitations on the other hand can be detected for concentrations up to 20% [42]. The excitation energies shift to higher energies ($\hbar\omega_{lib}/k_B = 50\,\mathrm{K}$ for $x=0.20$) and are heavily damped [42]. Very similar conclusions can be drawn from Raman work [43]. Here, the low-energy spectra and the side bands of the stretching modes have been studied at 10 K. In the glassy low-temperature state polarized spectra were analyzed. In a $(KBr)_{1-x}(KCN)_x$ mixed crystal with 2.5%

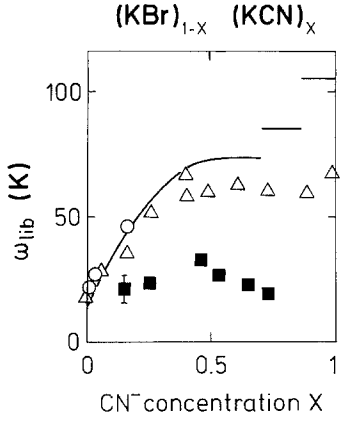


**Fig. 5.** Librational energies $\omega_{lib}$ (in units of Kelvin) calculated from the hindering barriers of Fig. 2 (solid lines) and as taken from neutron scattering (○, Ref. 42) and Raman experiments (△, Ref. 43). The closed squares were deduced from the excess specific heat of Fig. 4: (■)

**Table 1.** Parameters as derived from fits to the specific heat: Debye temperatures $\Theta_D$ (#: for pure KCN data taken from Ref. 39), scaling factors $S^{-1}$, mean librational frequencies of the $CN^-$ ions $\omega_{lib}$ and the distribution widths of the librational modes $\sigma_{lib}$ (FWHM). Parameters calculated from the results of the dielectric measurements: librational frequencies $\omega_{lib}^{calc}$, distribution widths of the librational frequencies $\sigma_{lib}^{calc}$ (FWHM), and the density of tunneling states $P(x, t=1\,s)$ times the asymmetry parameter $\Delta = k_B$ 340 K [9, 28]

| $X_{CN}$ | $\Theta_D$ [K] | $S^{-1}$ | $\omega_{lib}$ [K] | $\sigma_{lib}$ [K] | $\omega_{lib}^{calc}$ [K] | $\sigma_{lib}^{calc}$ [K] | $P(x, t=1\,s)\cdot\Delta$ [1/cm$^3$] |
|---|---|---|---|---|---|---|---|
| 0 | 174 | – | – | – | – | – | – |
| 0.008 | 170 | – | – | – | – | – | $4.4\ 10^{19}$ |
| 0.05 | 165 | – | – | – | – | – | $1.3\ 10^{20}$ |
| 0.15 | 158 | 3 | 21 | 10.8 | 42.6 | 22 | $9.9\ 10^{19}$ |
| 0.23 | 157.5 | 6 | 22 | 8.7 | 52.2 | 21 | $4.1\ 10^{19}$ |
| 0.46 | 152 | 2.8 | 34 | 9.4 | 72.1 | 20 | $1.1\ 10^{18}$ |
| 0.53 | 150 | 8.5 | 27 | 7.5 | 73.8 | 21 | $1.1\ 10^{18}$ |
| 0.65 | 157.5 | 17 | 24 | 7.1 | 73.8 | 22 | $2.8\ 10^{18}$ |
| 0.73 | 156 | 28 | 21 | 4.7 | 105.8 | 23 | $1.1\ 10^{16}$ |
| 0.93 | 185 | – | – | – | – | – | – |
| 1.00 | 195 # | – | – | – | – | – | – |

$CN^-$ ions the lowest Raman band in $E_g$ symmetry appears at approximately 20 K, the band in $T_{2g}$ symmetry at 10 K [43]. With increasing concentration both excitations shift to higher energies and finally at $x=0.15$, the two frequencies coincide at an energy of about 35 K. For $0.4 \leqq x \leqq 0.95$ Raman bands are independent of concentration and are located near 60 K. The lowest bands in this concentration range have been interpreted as librational motion of isolated $CN^-$ defects. The intensities of these excitations reach a maximum near $x=0.90$ and then abruptly drop to zero. In pure KCN two librational excitations were identified at 190 K and at 270 K [43, 45, 46].

The librational energies calculated from (6) using the hindering barriers as determined from the dielectric experiments (Fig. 2) and an effective moment of inertia $I_{eff}=2.65\ 10^{-39}$ g cm$^2$ [30] are shown in Fig. 5. The experimental results from Raman and neutron scattering techniques are shown for comparison. Surprisingly, for concentrations $x \leqq 0.7$ the agreement is excellent. Deviations appear in the monoclinic phase and especially in the orthorhombic phase, where (6) predicts a librational energy of 105 K compared to 190 K as determined from the Raman experiments.

### *B. The excess specific heat*

In order to parametrize the specific heat data of Fig. 4 in terms of (1), the Debye specific heat was calculated according to

$$C_D = 18 N_L k_B \left(\frac{T}{\Theta_D}\right)^3 \int_0^{x_D} \frac{x^4 \exp(x)}{[\exp(x)-1]^2}\,dx, \tag{10}$$

with $x_D = \hbar\omega_D/(k_B T)$. The Debye temperatures $\Theta_D$ as given in Table 1 were fitted to the high-temperature tail ($T \gtrsim 15$ K) of the $C_p$-data of Fig. 4. The excess specific heat, which appears as a bump in $C_p/T^3$ versus $T$, was

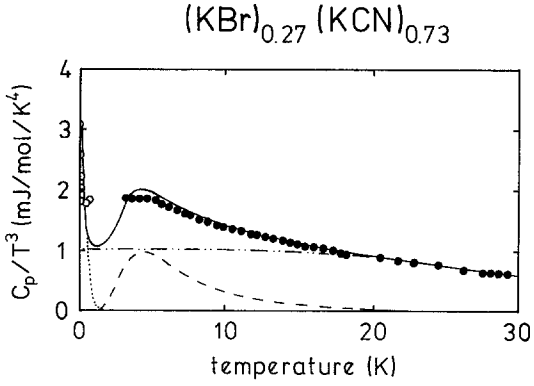


**Fig. 6.** Representative result for the fit to the low-temperature specific heat of $(KBr)_{0.27}(KCN)_{0.73}$ as described in the text: (●) this work; $x=0.70$ (○) from Ref. 5. While the Debye specific heat is represented by the dashed-dotted line, the dotted line and the dashed line depict the linear and the excess contributions, respectively. The sum of the three terms is represented by the full line

described according to Sethna's model [9, 10] by a distribution of librational modes. Harmonic librations can be described by an Einstein-type of specific heat, namely

$$C_E = S \frac{2 N_L k_B}{\sigma'_{lib}\sqrt{2\pi}} \int_0^{\infty} \left(\frac{\Theta_E}{T}\right)^2 \frac{\exp(\Theta_E/T)}{(\exp(\Theta_E/T)-1)^2} \cdot \exp\left[\frac{-(\Theta_E-\Theta_E^0)^2}{2\sigma'^2_{lib}}\right] d\Theta_E. \tag{11}$$

The Einstein temperature $\Theta_E^0$ corresponds to a librational energy $\omega_{lib} = k_B \Theta_E^0/\hbar$. The scale factor $S$ accounts for the fraction of oscillating $CN^-$ ions. $S$, $\omega_{lib}$, and $\sigma'_{lib}$ were treated as fitting parameters. A representative result of the quality of these fits with parameters given in Table 1 is shown in Fig. 6. Here the linear, the excess, and the Debye term are plotted separately. The specific heat data for $T<1$ K were taken from Ref. 5. Model calcula-

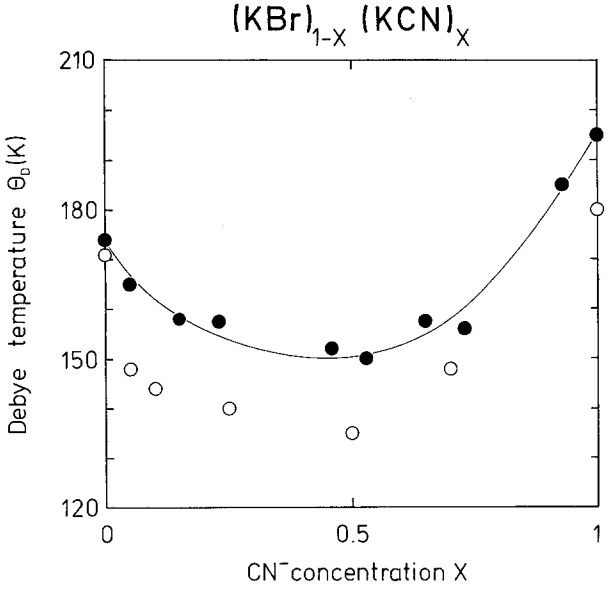


**Fig. 7.** Concentration dependence of the Debye temperatures $\Theta_D$ in $(KBr)_{1-x}(KCN)_x$ as obtained by fits to the specific heat data (●) (see also Table 1) and as determined from low-$T$ elastic constants (○) by De Yoreo et al. [5]. The value for $x=1.00$ was calculated using data from Ref. 39. The line is drawn to guide the eye

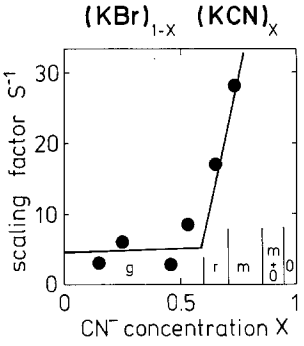


**Fig. 8.** Inverse scale factor $S^{-1}(x)$ obtained from fits to the specific heat. The line is drawn to guide the eye. Vertical lines indicate phase boundaries as in Fig. 2

tions and experimental results are in reasonable agreement. The Debye temperature ($\Theta_D=156$ K) is in the expected order of magnitude. However, the librational energy ($\omega_{\text{lib}}=21$ K) seems to be too small by a factor of three. The scale factor ($S=0.036$) appears to be unrealistically small.

The concentration dependence of the fitting parameters $\omega_{\text{lib}}$, $\Theta_D$, and $S^{-1}$, as derived from the fits to the specific heat data for concentrations $0.15<x<0.73$, are shown in the Figs. 5, 7, and 8, respectively and are listed in Table 1. The concentration dependence of the Debye temperature (Fig. 7) is in reasonable agreement with results as calculated from the low-temperature elastic constants [5, 29]. (The values of $\Theta_D$ as calculated from the elastic constants cited in Ref. 5 are also shown in Fig. 7. See also Ref. 47.) However, we believe that the values derived here are more realistic due to the fact that the elastic behaviour exhibits an anomalous temperature and a strong frequency dependence [3]. Hence, it is difficult to extrapolate the elastic behaviour to the quasi-static time scale of a specific heat experiment. In addition, the data on the elastic constants are incomplete: even in the pseudo-cubic glassy low-$T$ state, values of $c_{12}$ and $c_{11}$ have hardly been measured. In the non-cubic phases elastic constants are not available due to the multidomain state.

The librational energies plotted in Fig. 5 can be compared directly to calorimetric results of the lowest lying librational modes in $(KBr)_{1-x}(KCN)_x$: the librational energies as derived from the excess specific heat are almost independent of $x$. Of course this is only a parametrization of the fact that the maxima of the excess contributions to the specific heat are nearly concentration independent. It documents that, like in canonical glasses, the excess contribution does not depend on structural details.

The mean libration frequency $\omega_{\text{lib}}$ was calculated with the dielectric results using the effective moment of inertia per $CN^-$ molecule [30] which was assumed to be independent of concentration. This is plausible, since the effective moment of inertia represents the strength of the rotation-translation-coupling, which increases linearly with concentration. Thus, for a given host lattice, the effective mass per $CN^-$ molecule should be constant for all concentrations. Figure 5 raises some doubts concerning the suggestions of Randeria and Sethna [10] that the excess specific heat is due to an isolated librational motion of the $CN^-$ dumbbells. However, it remains to be demonstrated to what extent a more realistic model [11] including rotation-translation coupling yields a better agreement with the experimental results.

The mean distribution widths of the librational modes ($\sigma_{\text{lib}}$) which result from the analysis of the heat capacity results are listed in Table 1 and are compared to $\sigma_{\text{lib}}^{\text{calc}}$ as calculated from the dielectric measurements. The latter are almost independent of concentrations ($\sigma_{\text{lib}}^{\text{calc}}\approx 20$ K), while the former decreases from 11 K ($x=0.15$) to 5 K ($x=0.73$). The FWHM of the lowest librational mode as observed by inelastic neutron scattering amounts $\approx 30$ K ($x=0.16$) [42].

A clear indication against the assumption that the excess contribution is due to a single ion librational motion comes from the concentration dependence of the scale factor. The concentration dependence of the inverse scale factor $S^{-1}(x)$ is shown in Fig. 8 (see also Table 1). In the glassy state the scale is almost independent of concentration. Only a fraction of approximately 30% of the CN molecules contributes to the excess specific heat, if librational motion is assumed. This result is in agreement with neutron scattering results where it has been demonstrated that at the glass transition the librational degrees of freedom are reduced significantly [42]. In the ordered phases $S^{-1}$ strongly increases. However, small angle single ion oscillations should be possible in the glassy state as well as in the elastically ordered phases. We feel, that the results as presented in Figs. 5 and 8 are in direct conflict with the hypothesis that the $C_{\text{exc}}$ term results from librational modes. Once again,

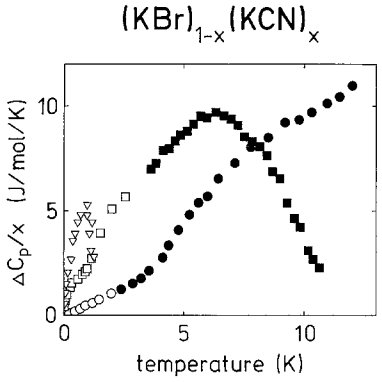


**Fig. 9.** Rotational low-temperature specific heat $\Delta C_p/x$ for $(KBr)_{1-x}(KCN)_x$ concentrations $x=0.15‰$ (V, Ref. 48); $x=8‰$ (■, this work including data from [49]; □, after Ref. 50) and $x=5\%$ (●, this work; ○, from Ref. 5). The Debye specific heat due to the phonon background has been subtracted from the experimentally determined specific heat

it should be pointed out that a model is needed which tries to give an explanation for the experimental fact that all non-crystalline solids exhibit a very similar excess contribution to the specific heat, independent of structural details as well as of the vibrational spectra. In this respect the new approach from Schirmacher and Wagener [24] deserves attention: in their model, $C_{exc}$ is a direct consequence of disorder only and a bump appears in $C_p/T$ near $T/\Theta_D=0.03$ in rough agreement with our results. We suggest, that the results of Fig. 8 give a measure of the degree of disorder of the system (or a measure of the fraction of disordered regions). Obviously in the monoclinic phases the disorder is restricted to the domain walls and thus only to a minor fraction of the total sample volume.

### *C. The low-temperature specific heat in the dilute limit*

In this chapter we comment on the low-temperature specific heat in $(KBr)_{1-x}(KCN)_x$ mixed crystals for concentrations ranging from the very dilute limit ($x<1‰$) up to the low concentration regime ($x\approx 5\%$). Some of the experimental results are depicted in Fig. 9. The specific heat in the 0.15‰ crystal was measured by Peressini [48]. The data for the 0.8% sample are shown together with data from Mertz and Loidl [49]. Here we added new results from literature for low temperatures ($T<2$ K) [50]. In Fig. 9 we plotted the rotational specific heat $\Delta C_p$ which was obtained by subtracting the phonon contributions from the experimental results normalized to the $CN^-$ concentration $x$. For the crystals with concentrations $x<0.05$ the specific heat of pure KBr was subtracted (Fig. 9). For $(KBr)_{0.992}(KCN)_{0.008}$ and $(KBr)_{0.95}(KCN)_{0.05}$ the phonon background could also be calculated with Debye temperatures of 170 K and 165 K, respectively (see Fig. 7).

For the sample with $x=0.15‰$ the specific heat exhibits a well-defined Schottky-type anomaly which is due to a tunnel-split groundstate. A neutron scattering study by Rowe et al. [41] located a tunneling transition in $(KBr)_{1-x}(KCN)_x$ with $x=34‰$ at 3.2 K. The solid solution with a concentration of $x=0.8\%$ shows a broad maximum in $\Delta C_p$ at 5 K. Obviously, already in a 0.8% sample the effective $CN^- - CN^-$ interactions are strong enough to suppress any well-defined tunneling or rotational excitation. In a neutron scattering study by Loidl et al. [42] the tunneling transition in this crystal was located near 3 K. However, it has been shown that only a small fraction of $CN^-$ ions contributes to this excitation. It was argued that the active tunneling centers are situated in the cubic crystal field (zero random strain), while the majority of molecules was thought to be exposed to a distribution of random strain fields which results from the site disorder and the anisotropic quadrupole-quadrupole interaction. It is unclear whether the bump near 0.5 K ($x=0.8\%$) is significant, since due to the subtraction procedure the experimental error is rather large. In this context it is interesting to mention that one decade ago Fischer and Klein [44] calculated the specific heat of strain defects in alkali halides. They proposed a glass-like specific heat which arises purely from strain mediated interactions between tunneling units. Their calculations predict a small peak in the specific heat near the energy of the tunnel splitting and a linear increase for further increasing temperatures which roughly agrees with the rotational specific heat of the 0.8% sample below 5 K. Finally, the 5% sample exhibits an extraordinarily strong, almost linear increase of the rotational specific heat for $T<15$ K. From the dielectric measurements (Figs. 2 and 3) we know that the mean hindering barrier in this sample is approximately 70 K with a distribution width of 190 K. Thus, a large fraction of $CN^-$ ions experiences very low quadrupolar fields (an almost vanishing hindering barrier) and effectively contributes to the low-temperature specific heat.

### *D. The linear term in the specific heat*

Finally, we calculated the linear term of the specific heat in the framework of Sethna's model [9]. With the results from the dielectric investigation, we now compute the density of tunneling states $P(t)\cdot\Delta$ using (4). The concentration dependence of this product is shown in Fig. 10 (see also Table 1). Near $x=0.1$ a peak shows up, with a continuous decrease for further increasing concentrations $x$. At the rhombohedral to monoclinic phase boundary a sharp drop becomes apparent and the density of tunneling states is reduced by a factor of 100. The results shown in Fig. 10 reveal that a rhombohedral glass exists in addition to the cubic glass phase. The existence of non-cubic glassy phases in $(KBr)_{1-x}(KCN)_x$ mixed crystals has been predicted by Lewis and Klein [51] on the basis of molecular dynamics calculations. The nomenclature cubic or rhombohedral glass refers to the mean long range order of the center of mass lattice. Short range order correlations due to frozen-in local shear distortions are superimposed on this topological order. It seems important that the rhombohedral phase is characterized by partial quadrupolar order only. At

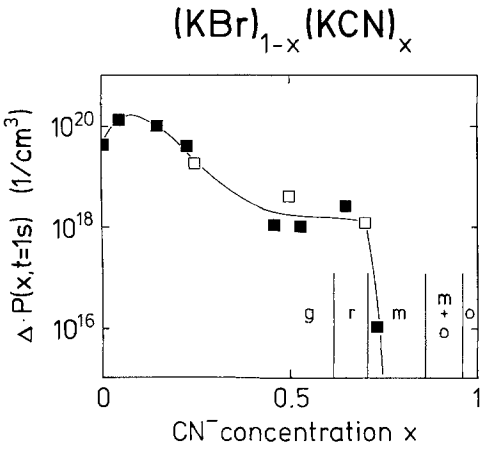


**Fig. 10.** Concentration dependence of the density of tunneling states times asymmetry ($P(t=1\,s)\cdot\Delta$) as calculated from parameters determined by dielectric spectroscopy in $(KBr)_{1-x}(KCN)_x$ (■, this work) and determined from calorimetric results for $\bar{P}$ cited from Ref. 5 and multiplied with the constant $\Delta = k_B$ 340 K [8, 28] (□). The vertical lines indicate boundaries between regions where the samples show different crystallographic structures (see Fig. 2). The solid line is drawn to guide the eye

the cubic to rhombohedral glass transition the quadrupolar degrees of freedom are reduced from 4 to 3 [31, 37]. Hence, a quadrupolar freezing process still may occur yielding the low-temperature glass state.

A comparison with experimental results from the low-temperature specific heat is possible only, if assumptions concerning the asymmetry parameter $\Delta$ are made. Here we followed the suggestions of Refs. 9 and 28 and took $\Delta = k_B$ 340 K to be constant for all concentrations. This value represents the asymmetry of the reorientational potential in KCN [28]. Under these assumptions the agreement between the calculated and the measured [5] linear term of the specific heat is excellent (Fig. 10 and Table 1). For $x=0.25$, 0.5 and 0.75 this has been demonstrated already previously [28].

It has been demonstrated by Nicholls et al. [52] that in solid solutions of $N_2$:Ar:CO dipolar interaction forces are not essential for the appearance of a linear term in the specific heat. We interpret this result as a hint that the asymmetry caused by dipolar interaction forces is of minor importance in this system. A generalization of this conclusion would be in conflict with the importance which the asymmetry energy $\Delta$ plays in $(KBr)_{1-x}(KCN)_x$.

## V. Conclusions

The main conclusions that can be drawn from this dielectric and thermodynamic investigation of the orientational glass $(KBr)_{1-x}(KCN)_x$ can be summarized as follows:

– the hindering barriers of the reorientational potential of the $CN^-$ molecules increase roughly linearly with $x$. However, to some degree $E_0(x)$ reflects the symmetry of the low-temperature state (Fig. 2).

– the distribution of barriers is a smooth function of $x$, with maximum widths appearing at intermediate concentrations. Surprisingly, $\sigma_x$ is broader in the orthohombic and monoclinic phases than in the glass state near the critical concentration

– for $0.1 \leqq x \leqq 0.73$ $(KBr)_{1-x}(KCN)_x$ exhibits glassy low-temperature anomalies, i.e. both, a linear [5] and an excess contribution to the specific heat.

– for $x \leqq 0.1$ the specific heat is highly anomalous as compared to the Debye specific heat of a crystalline solid, but is totally different from that as observed in canonical glasses.

– within the framework of the microscopic model, as proposed by Sethna et al. [9, 10], both the linear and the excess term were calculated from the crystal field parameters determined by dielectric spectroscopy. The agreement between the calculated and the experimentally observed [5] linear term of the specific heat is excellent. However, the excess contribution is not satisfactorily described within this model. We feel that any model for $C_{exc}$ must be independent of structural details and independent of the vibrational spectrum of the glass.

– the calculated density of tunneling states in $(KBr)_{1-x}(KCN)_x$ demonstrates that the cubic as well as the rhombohedral phases exhibit glassy character.

This work has been supported by the Sonderforschungsbereich 262 "Glaszustand und Glasübergang nichtmetallischer amorpher Materialien" and by the Center for Material Research (Materialwissenschaftliches Forschungszentrum), Mainz. The work of one of us (B.M.) has been submitted in partial fulfillment of the requirements (D77) for the degree of Doctor rerum naturalium at the Johannes Gutenberg-Universität Mainz.

## References

1. Loidl, A.: Annu. Rev. Phys. Chem. **40**, 29 (1989)
2. Lüty, F.: In: Defects in insulating crystals. Turkevich, V.M., Svarts, K.K. (eds.), pp. 69–89. Berlin, Heidelberg, New York: Springer 1981
3. Volkmann, U.G., Böhmer, R., Loidl, A., Knorr, K., Höchli, U.T., Haussühl, S.: Phys. Rev. Lett. **56**, 1716 (1986); Loidl, A., Knorr, K.: NY Acad. Sci. **484**, 121 (1986)
4. Doverspike, M.A., Wu, M.C., Conradi, M.S.: Phys. Rev. Lett. **56**, 2284 (1986)
5. DeYoreo, J.J., Knaak, W., Meissner, M., Pohl, R.O.: Phys. Rev. **34**, 8828 (1986); DeYoreo, J.J., Meissner, M., Pohl, R.O., Rowe, J.M., Rush, J.J., Susman, S.: Phys. Rev. Lett. **51**, 1050 (1983)
6. Berret, J.F., Doussineau, P., Levelut, A., Meissner, M., Schön, W.: Phys. Rev. Lett. **55**, 2013 (1985)
7. Moy, D., Dobbs, J.N., Anderson, A.C.: Phys. Rev. B**29**, 2160 (1984)
8. Baier, G., v. Schickfus, M., Enss, C.: Europhys. Lett. **8**, 487 (1989)
9. Sethna, J.P.: Physics Today **39**, S20 (1986); Sethna, J.P., Chow, K.S.: Phase Transitions **5**, 317 (1985); Meissner, M., Knaak, W., Sethna, J.P., Chow, K.S., DeYoreo, J.J.: Phys. Rev. B**32**, 6091 (1985); Sethna, J.P.: N.Y. Acad. Sci. **484**, 130 (1986)
10. Randeria, M.: Thesis (1987), Cornell University (unpublished); Randeria, M., Sethna, J.P.: Phys. Rev. B**38**, 12607 (1988)
11. Grannan, E.R., Randeria, M., Sethna, J.P.: Phys. Rev. Lett. **60**, 1402 (1988)

12. Zeller, R.C., Pohl, R.O.: Phys. Rev. B**4**, 2029 (1971);
Pohl, R.O.: In: Amorphous solids. Phillips, W.A. (ed.), pp. 27–51, Berlin, Heidelberg, New York: Springer 1981
13. Guided by the interpretation of low-$T$ specific heat data ($T \lesssim 2$ K) it became standard to describe the excess term by a $T^3$ dependence. However, the results of a number of glasses revealed that the excess contributions have a more complex temperature dependence and appear as a bump in a $C/T^3$ versus $T$ plot. In $(NaCN)_{1-x}(KCN)_x$ glassy solids the $T^3$ range extends to $T \approx 6$ K with no evidence of an excess bump; see Mertz, B., Berret, J.F., Böhmer, R., Loidl, A., Meissner, M., Knaak, W.: Phys. Rev. B (submitted for publication)
14. Anderson, P.W., Halperin, B.I., Varma, C.M.: Philos. Mag. **25**, 1, (1972)
15. Phillips, W.A.: J. Low Temp. Phys. **7**, 351 (1972)
16. Buchenau, U., Zhou, H.M., Nücker, N., Gilroy, K.S., Phillips, W.A.: Phys. Rev. Lett. **60**, 1318 (1988);
Buchenau, U.: Solid State Commun. **56**, 889 (1985)
17. Loponen, M.T., Dynes, R.C., Narayanamurti, V., Garno, J.P.: Phys. Rev. Lett. **46**, 265 (1981);
Loponen, M.T., Dynes, R.C., Narayanamurti, V., Garno, J.P.: Phys. Rev. B**25**, 1161 (1982)
18. Meissner, M., Spitzmann, K.: Phys. Rev. Lett. **46**, 265 (1981)
19. Dreyfuss, B., Fernandes, N.C., Maynard, R.: Phys. Lett. A**26**, 647 (1968)
20. Derrida, B., Orbach, R., Kin-Wah, Yu: Phys. Rev. B**29**, 6645 (1984)
21. Nagel, S.R., Grest, G.S., Feng, S., Schwartz, L.M.: Phys. Rev. B**34**, 8667 (1986)
22. Phillips, J.C.: Phys. Rev. B**24**, 1744 (1981)
23. Wang, Y.R.: J. Phys. Chem. Solids **47**, 181 (1986)
24. Schirmacher, W., Wagener, M.: In: Dynamics of disordered materials. In: Springer Proceedings in Physics. Richter, D., Dianoux, A.J., Petry, W., Teixeira, J. (eds.), Vol. 37, pp. 231–234. Berlin, Heidelberg, New York: Springer 1989
25. Knorr, K., Loidl, A.: Z. Phys. B – Condensed Matter **46**, 219 (1982)
26. Bhattacharya, S., Nagel, S.R., Fleishman, L., Susman, S.: Phys. Rev. Lett. **48**, 1267 (1982)
27. Birge, N.O., Jeong, Y.H., Nagel, S.R., Bhattacharya, S., Susman, S.: Phys. Rev. B**30**, 2306 (1984)
28. Wu, L., Ernst, R.M., Jeong, Y.H., Nagel, S.R., Susman, S.: Phys. Rev. B**37**, 10444 (1988);
Ernst, R.M., Wu, L., Nagel, S., Susman, S.: Phys. Rev. B**38**, 6246 (1988)
29. Watson, S.K., Cahill, D.G., Pohl, R.O.: Phys. Rev. B**40**, 6381 (1989)
30. Beyeler, H.U.: Phys. Rev. B**11**, 3078 (1975)
31. Loidl, A., Schräder, T., Knorr, K., Böhmer, R., Mertz, B., McIntyre, G.J., Vogt, T., Mutka, H., Müllner, M., Jex, H., Haussühl, S.: Z. Phys. B – Condensed Matter **75**, 81 (1989)
32. For details see: Eisele, B.: Diplomarbeit, Universität Mainz (1989) (unpublished);
Böhmer, R.: Diplomarbeit, Universität Main (1985) (unpublished)
33. Cole, K.S., Cole, R.H.: J. Chem. Phys. **9**, 341 (1941)
34. Sethna, J.P., Nagel, S.R., Ramakrishnan, T.V.: Phys. Rev. Lett. **53**, 2489 (1984)
35. Lüty, F., Ortiz-Lopez, J.: Phys. Rev. Lett. **50**, 1289 (1983);
Ortiz-Lopez, J.: Thesis (1986), University of Utah (unpublished)
36. Böhmer, R.: J. Chem. Phys. **91**, 3111 (1989)
37. Some of the crystals have been studied previously (Mertz, B., Loidl, A.: Europhys. Lett. **4**, 583 (1987); see also Ref. 49). The data presented in this work, were obtained in subsequent experiments and confirmed the previous results whenever possible.
38. Brockhouse, B.N., Iyengar, P.K.: Phys. Rev. **111**, 747 (1958)
39. Suga, H., Matsuo, T., Seki, S.: Bull. Chem. Soc. Jpn. **38**, 1115 (1965)
40. Walton, D., Mook, H.A., Nicklow, R.M.: Phys. Rev. Lett. **33**, 412 (1974)
41. Rowe, J.M., Rush, J.J., Shapiro, S.M., Hinks, D.G., Susman, S.: Phys. Rev. B**21**, 4863 (1980)
42. Loidl, A., Knorr, K., Feile, R., Kjems, J.K.: Phys. Rev. Lett. **51**, 1054 (1983);
Loidl, A., Feile, R., Knorr, K., Kjems, J.K.: Phys. Rev. B**29**, 6052 (1984)
43. Durand, D., Lüty, F.: Ferroelectrics **16**, 205 (1977);
Durand, D.: (unpublished, 1976)
44. Fischer, B., Klein, M.W.: Phys. Rev. Lett. **43**, 289 (1979)
45. Dultz, W.: Solid State Commun. **15**, 595 (1974)
46. Nücker, N., Knorr, K., Jex, H.: J. Phys. C**11**, 1 (1978)
47. The careful review of the elastic constants given in literature (see in Ref. 29) does not alter the Debye temperatures $\Theta_D$ significantly as compared to Ref. 5
48. Peressini, P.P.: Thesis (1973), Cornell University (unpublished)
49. Mertz, B., Loidl, A.: J. Phys. C**18**, 2843 (1985)
50. Knaak, W., Meissner, M.: In: Disordered systems and new materials. Borissov, M., Kirov, N., Vavrek, A. (eds.), pp. 399–415. Singapore, New Jersey, London, Hong Kong: World Scientific 1989
51. Lewis, L.J., Klein, M.L.: Phys. Rev. Lett. **59**, 1837 (1987)
52. Nicholls, C.I., Yadon, L.N., Haase, D.G., Conradi, M.S.: Phys. Rev. Lett. **59**, 1317 (1987)

B. Mertz, R. Böhmer, B. Eisele, A. Loidl
WA KOMA
Institut für Physik der Universität
Staudinger Weg 7
D-6500 Mainz
Federal Republic of Germany